

Light-Controlled Delivery of Monoclonal Antibodies for Targeted Photoinactivation of Ki-67

Sijia Wang,^{†,‡,§} Gereon Hüttmann,[‡] Zhenxi Zhang,[†] Alfred Vogel,[‡] Reginald Birngruber,[‡] Shifalika Tangutoori,^{||} Tayyaba Hasan,^{||} and Ramtin Rahmanzadeh^{*‡}

[†]Key Laboratory of Biomedical Information Engineering of Ministry of Education, Institute of Biomedical Analytical Technology and Instrumentation, School of Life Science and Technology, Xi'an Jiaotong University, Xi'an 710049, P. R. China

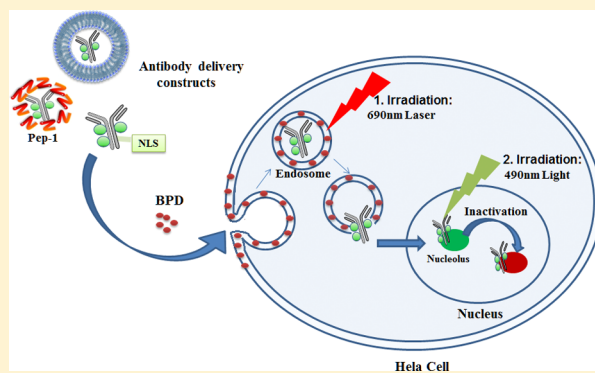
[‡]Institute of Biomedical Optics, University of Lübeck, Peter-Monnik-Weg 4, 23562 Lübeck, Germany

^{||}Wellman Center for Photomedicine, Massachusetts General Hospital, Harvard Medical School, 50 Blossom Street, Boston, Massachusetts 02114, United States

Supporting Information

ABSTRACT: The selective inhibition of intracellular and nuclear molecules such as Ki-67 holds great promise for the treatment of cancer and other diseases. However, the choice of the target protein and the intracellular delivery of the functional agent remain crucial challenges. Main hurdles are (a) an effective delivery into cells, (b) endosomal escape of the delivered agents, and (c) an effective, externally triggered destruction of cells. Here we show a light-controlled two-step approach for selective cellular delivery and cell elimination of proliferating cells. Three different cell-penetrating nano constructs, including liposomes, conjugates with the nuclear localization sequence (NLS), and conjugates with the cell penetrating peptide Pep-1, delivered the light activatable antibody conjugate TuBB-9-FITC, which targets the proliferation associated protein Ki-67. HeLa cells were treated with the photosensitizer benzoporphyrin monoacid derivative (BPD) and the antibody constructs. In the first optically controlled step, activation of BPD at 690 nm triggered a controlled endosomal escape of the TuBB-9-FITC constructs. In more than 75% of Ki-67 positive, irradiated cells TuBB-9-FITC antibodies relocated within 24 h from cytoplasmic organelles to the cell nucleus and bound to Ki-67. After a second light irradiation at 490 nm, which activated FITC, cell viability decreased to approximately 13%. Our study shows an effective targeting strategy, which uses light-controlled endosomal escape and the light inactivation of Ki-67 for cell elimination. The fact that liposomal or peptide-assisted delivery give similar results leads to the additional conclusion that an effective mechanism for endosomal escape leaves greater variability for the choice of the delivery agent.

KEYWORDS: *liposome, nuclear localization sequence (NLS), nanotechnology, endosomal entrapment, photodynamic therapy*



1. INTRODUCTION

Molecular targeted therapies are promising approaches for cancer treatment.¹ Many possible targeting agents block or interrupt specific pathways involved in tumor growth and cancer cell proliferation.² Selectively inactivating a cellular molecule will combine optimal treatment outcome with low or even no systemic side effects. From many targets that have been investigated, only the inhibition of cell surface or secreted molecules, like, e.g., EGFR,³ HER2^{4,5} or VEGF,⁶ and intracellular non-nuclear proteins, targeted with small molecular drugs, are in clinical use. However, many proteins that are emerging as interesting targets for therapies have intracellular and nuclear localization, which makes an efficient delivery of targeting moieties, especially if they are macromolecules, extremely challenging.⁷

The nuclear protein Ki-67 is a compelling candidate for molecular targeted therapy. It is strongly expressed in

proliferating cells^{8,9} and is an established prognostic indicator for the assessment of cell proliferation in biopsies from cancer patients.¹⁰ The monoclonal antibody TuBB-9 specifically recognizes a physiologically active form of Ki-67, which localizes with the antibody in the nucleus.¹¹ In prior work we established the ability of TuBB-9 FITC conjugates to selectively and efficiently kill proliferating cancer cells after light irradiation by the production of singlet oxygen and other reactive oxygen species.^{12,13} Building on that work we show a new strategy for uptake of cell-penetrating nanoconstructs that make nuclear localization of macromolecular IgG antibodies more efficient and controllable.

Received: April 2, 2015

Revised: June 29, 2015

Accepted: July 30, 2015

Published: July 30, 2015

Diverse delivery vehicles like liposomes,⁵ cell-penetrating peptides (CPPs),¹⁴ polymer constructs,¹⁵ or viral vectors¹⁶ have been established to facilitate transport of macromolecules across the cellular membrane. In these methods, the delivery efficacy of the vehicles is often dependent on the structure of the target molecule and the cell type. They are efficient in the delivery of structurally uniform materials, such as nucleic acids, but often not as successful for the delivery of larger molecules with more complex structures, such as antibodies.^{17,18} Moreover, most of these vehicles are taken up by cells via endocytosis, especially when used with macromolecules.¹⁹ Endocytosed agents will mostly stay trapped in endosomes and lysosomes, and will there be exposed to the acidic environment and degrading enzymes. In the end the delivered molecules are often degraded instead of exerting their therapeutic action in the cell.^{20,21} Therefore, besides an efficient delivery inside cells the escape from the endosomal vesicles and release into the cytoplasm is essential for the successful intracellular delivery of macromolecules.

For our study we use a liposomal formulation of TuBB-9-FITC, a conjugate of TuBB-9 with the cell penetrating peptide (CPP) Pep-1 and a conjugate of TuBB-9 with the nuclear localization sequence (NLS) from the SV-40 virus (Figure 1).

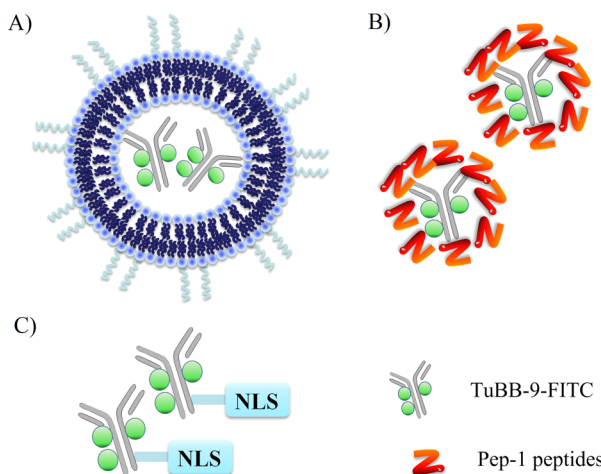


Figure 1. Diagram of the different antibody constructs used for targeting the Ki-67 protein. (A) TuBB-9-FITC encapsulated in liposomes, (B) Pep-1 sequences noncovalently bound to TuBB-9-FITC, and (C) TuBB-9-FITC conjugated to NLS by a SMCC linker.

Liposomes are self-assembling spherical vesicles synthesized of lipids, which enable an intracellular delivery of large macromolecules. Several liposomal drugs have already been approved for clinical use.²² Pep-1 sequences improve the delivery of proteins and peptides in their biologically active form into a variety of cell lines, without the need for prior chemical covalent coupling steps.²³ NLS binds to *Importin* proteins, which are actively transported into the nucleus via nuclear pores. Macromolecules conjugated to NLS have been successfully transported into the nucleus.²⁴

For a light triggered endosomal escape we use the lipophilic photosensitizing porphyrin benzoporphyrin derivative mono-acid (BPD). Lipophilic and amphiphilic porphyrins or porphyrin-related compounds localize primarily in cellular membranes.²⁵ Upon illumination with light, photosensitizers generate singlet oxygen and other reactive oxygen species (ROS).²⁶ These ROS have a short lifetime (<0.04 μs) and short

range of action (<20 nm)²⁷ so that most of the damaging effects are limited to the endosomal membrane. ROS disrupt the endosome by oxidizing its membrane constituents and thus facilitate the passage of trapped therapeutic macromolecules into the cytoplasm.²⁸

Here we demonstrate for three different constructs that endosomal entrapment can be overcome by light activation of BPD and show the free availability of the TuBB-9-FITC antibody in the cytoplasm. The antibody can then exert its action and effectively eliminate Ki-67 positive tumor cells.

2. EXPERIMENTAL SECTION

2.1. Antibodies and Labeling. The monoclonal mouse antibody TuBB-9 was produced from hybridoma cells kindly provided by Leibnitz Institute Borstel, Germany. Hybridoma cells were cultivated in bioreactor cell culture flasks (INTEGRA Biosciences, Switzerland). The antibodies were purified from the culture supernatant with protein G columns. As a control antibody we used the monoclonal antibody Erbitux against EGFR (Merck, Germany). For labeling with FITC (fluorescein 5(6)-isothiocyanate, Sigma, USA), antibodies (1 mg/mL in sodium carbonate buffer at pH 9.3) were mixed with FITC (2.57 mM in DMSO) in a molar ratio of 20:1. The solution was incubated at room temperature on a shaker for 2 h, and the labeled protein was purified with a NAP-5 Sephadex column (GE Healthcare). After elution with TBS (10 mM Tris-HCl at pH 8.2, 150 mM NaCl), the labeled antibodies were concentrated with Microcon tubes (Millipore, USA) and resuspended in TBS (pH 7.4). Between 1.5 and 2.4 molecules of FITC were bound to each antibody.

2.2. Preparation and Characterization of L-TuBB-9-FITC. Liposomes for encapsulating TuBB-9-FITC (L-TuBB-9-FITC) and Erbitux-FITC (L-Erbtitux-FITC) were prepared by dissolving the lipids DPPC, DOTAP, cholesterol, and PEG2000-DSPE (Avanti Polar Lipids, USA) in chloroform, in a ratio of 15:3:4:3. Chloroform was evaporated from the vial under a stream of nitrogen. The residual chloroform was removed by placing the vial in a desiccator under vacuum for 8 h. 500 μL of antibody-FITC conjugates at a concentration of 4 mg/mL was then added at 50 °C, a temperature greater than the highest fluid–solid transition temperature (T_m : 48 °C) of the lipids in the mixture. The solution was incubated for 30 min at 50 °C, gently mixed, and then transferred to ice. After 10 min the solution was incubated again for 10 min in the 50 °C water bath; these steps were repeated 6 times.

The resulting dispersion of multilamellar vesicles was extruded through a 100 nm polycarbonate membrane by using a mini-extruder system (Avanti Polar Lipids, USA) to form unilamellar vesicles. A CL-4B Sephadex column was used to remove unencapsulated antibody-FITC conjugates. The resulting liposomes were analyzed by dynamic light scattering (DLS) and transmission electron microscopy (TEM), and the concentrations of encapsulated antibody conjugates were determined by fluorescence and absorbance spectroscopy. Liposomes were stored at 4 °C, and DLS measurements and TEM images remain consistent at least for 4 weeks after preparation.

2.3. Conjugation of TuBB-9-FITC with NLS Peptides. Cysteine modified NLS (CGGGPKKKVED, Anaspec, USA) was conjugated to TuBB-9-FITC and Erbitux-FITC by referring to the method described by Chen and colleagues²⁹ using the linker molecule sulfosuccinimidyl-4-(N-maleimidomethyl)cyclohexane-1-carboxylate (sulfo-SMCC;

Pierce Chemical Co., USA). The maleimide groups were introduced to the antibody-FITC conjugates by the reaction of 3 mg of antibody-FITC conjugates with 0.18 mg of sulfo-SMCC in phosphate buffered saline (PBS, pH 7.4) in a ratio of 1:20 at room temperature for 1 h. The maleimide-derivatized antibody-FITC conjugates were then purified on a NAP-5 minicolumn (exclusion limit 5 kDa; GE Healthcare, USA) eluted with PBS, pH 7.0. The fractions containing maleimide antibody-FITC conjugates were transferred to an ultrafiltration device (100 kDa cutoff; Amicon, USA). The device was centrifuged at 800g for 20 min to concentrate maleimide-antibody-FITC to 2 mg/mL, which were then mixed with a 60-fold molar excess of NLS-peptides (10 mg/mL in PBS, pH 7.0) for 18 h at 4 °C. NLS-antibody-FITC conjugates were purified from excess NLS-peptides and concentrated to 2 mg/mL in PBS, pH 7.4, by ultrafiltration.

NLS-TuBB-9-FITC and NLS-Erbbitux-FITC were analyzed by sodium dodecyl sulfate-2-polyacrylamide gel electrophoresis (SDS-PAGE) under nonreducing conditions on a 5% Tris-HCl ready-minigel (Bio-Rad, USA) stained with Coomassie Brilliant Blue. The migration distance in the gel relative to the bromphenol blue dye front (R_f) was measured, and the numbers of NLS-peptides bound to the antibody-FITC conjugates were estimated.

2.4. Conjugation of TuBB-9-FITC with Pep-1 Peptides.

Pep-1-TuBB-9-FITC complex was prepared by mixing antibodies with Pep-1 peptides (KETWWETWWTEWSQPKKKRKVC, Anaspec, USA) before use, according to Morris et al.²³ Briefly, Pep-1 peptides (150 μL of 0.1 mg/mL in PBS) were treated by ultrasound for 5 min, incubated with 150 μL of TuBB-9-FITC (0.15 mg/mL) for 30 min at room temperature, and added to the cells. The Pep-1-TuBB-9-FITC complex was characterized by native polyacrylamide gel electrophoresis (Native-PAGE) under nonreducing conditions on a 5% Tris-HCl ready-minigel (Bio-Rad, USA) stained with Coomassie Brilliant Blue.

2.5. Cell Culture. Human cervical cancer cell line (HeLa) and Human ovarian adenocarcinoma cell line (OVCAR-3) were obtained from American Type Culture Collection (ATCC). Human dermal fibroblasts were obtained from the University Hospital Lübeck (UKSH, Lübeck, Germany). HeLa cells were maintained in Dulbecco's modified Eagle's medium (DMEM low glucose, Sigma, USA) containing 10% fetal bovine serum (FBS gold, PAA, USA) and 1% penicillin/streptomycin (PAA, USA). OVCAR-3 cells were cultured in RPMI-1640 medium (Sigma, USA) containing 10% FBS and 1% penicillin/streptomycin. Fibroblast cells were maintained in DMEM medium (high glucose, Sigma, USA) containing 10% FBS and 1% penicillin/streptomycin. Cells were incubated in humidified atmosphere at 37 °C with 5% CO₂. For measuring TuBB-9-FITC cellular uptake and the demonstration of the photochemical induced endosomal escape, 4×10^4 cells/mL were seeded in 35 mm Petri dishes.

2.6. Cellular Uptake and Localization of the TuBB-9-FITC Constructs. Cellular uptake and localization of the antibody conjugates and BPD were observed in HeLa cells by fluorescence microscopy (TE-Eclipse, Nikon, Japan). Cells were seeded with a concentration of 4×10^4 cells/mL on glass bottom imaging dishes or 96-well plates. Samples with the different delivery systems were adjusted to the same amount of antibody (15 μg/mL), and same incubation times (4 h) were used to obtain comparable results.

The amount of the internalized TuBB-9-FITC constructs in cells was determined by measuring the total fluorescence per well of the cells seeded on the 96-well plates in a multimode microplate reader (Spectramax M4, Molecular Devices, USA). After 4 h incubation with 3 μg of antibody per well (15 μg/mL), the cells were washed once with serum-free medium and twice with PBS. Cells were subsequently incubated with 100 mL of RIPA lysis buffer for 10 min at 20 °C. The lysates were homogenized by pipetting up and down five times. The fluorescence signal was measured in the microplate reader in 96-well plates in at least 12 independent experiments. The internalized amount of antibody was calculated from the mean fluorescence. Error bars represent standard deviation.

2.7. BPD Incubation and Endosomal Release. 18–20 h after seeding of 4×10^4 HeLa cells/cm² in DMEM containing 200 nM BPD (benzoporphyrin derivative monoacid Ring A, Sigma, USA) in glass bottom imaging dishes, the cells were washed twice with PBS and incubated for 4 h with 15 μg/mL TuBB-9-FITC construct. Then the cells were washed once with serum-free DMEM and twice with PBS. Light irradiation for ROS production and endosome disruption was performed with a 690 nm continuous wave diode laser (device built by Medical Laser Center, Lübeck, Germany) with 8 mW/cm² for 60 s. Fluorescence microscopy 5 min before and 5 min, 24, and 48 h after this PCI irradiation was used to observe the release from endosome and relocation of the TuBB-9-FITC conjugates.

2.8. Cell Viability Assay. HeLa cells were seeded at a density of 4×10^4 cells/mL in 96-well plates, 200 nM BPD was added into each well, and the cells were incubated for 20 h. Then, cells were incubated for another 4 h with the different constructs (TuBB-9-FITC, L-TuBB-9-FITC, NLS-TuBB-9-FITC, Pep-1-TuBB-9-FITC, Erbitux-FITC, L-Erbbitux-FITC, NLS-Erbbitux-FITC, Pep-1-Erbbitux-FITC). In all incubations a total amount of 3 μg of antibody per well (15 μg/mL) was used. After incubation, the cells were washed twice with PBS, and wells were divided into four groups: (1) no light irradiation, (2) irradiation with 690 nm laser for endosomal escape (8 mW/cm², 200 s), (3) incubation for 48 h and irradiation at 490 nm with a LED array for photoinactivation of Ki-67 (20 mW/cm², 3 min), and (4) irradiation at 690 nm and after 48 h a second irradiation at 490 nm for endosomal escape and photoinactivation of FITC. After treatment, some samples were stained with propidium iodide and calcein AM (Invitrogen, USA) for observation of cell viability under the fluorescence microscope. Other samples were incubated for 72 h and prepared for the MTT viability assay. After 72 h, cells were washed twice with PBS and 100 μL of MTT solution (1 mg/mL in culture medium) was added per well. After an additional incubation for 1 h, culture medium was removed and the samples were incubated in 200 μL of DMSO for 30 min on a shaker to dissolve the formazan crystals. Absorbance was measured on a microplate reader (Spectramax MS, Molecular Devices, USA) at 570 nm. Measured absorbance of treated samples compared to untreated controls was used as a measure for cell viability. Statistical analysis was performed by using SPSS (IBM Deutschland GmbH). The viability data of different groups were expressed as mean value and standard deviation of in total eight measurements. Student's *t*-test was used, and differences were considered significant at *p* < 0.05. To establish the growth curves of the different treatment groups, cells were counted during and after the treatment.

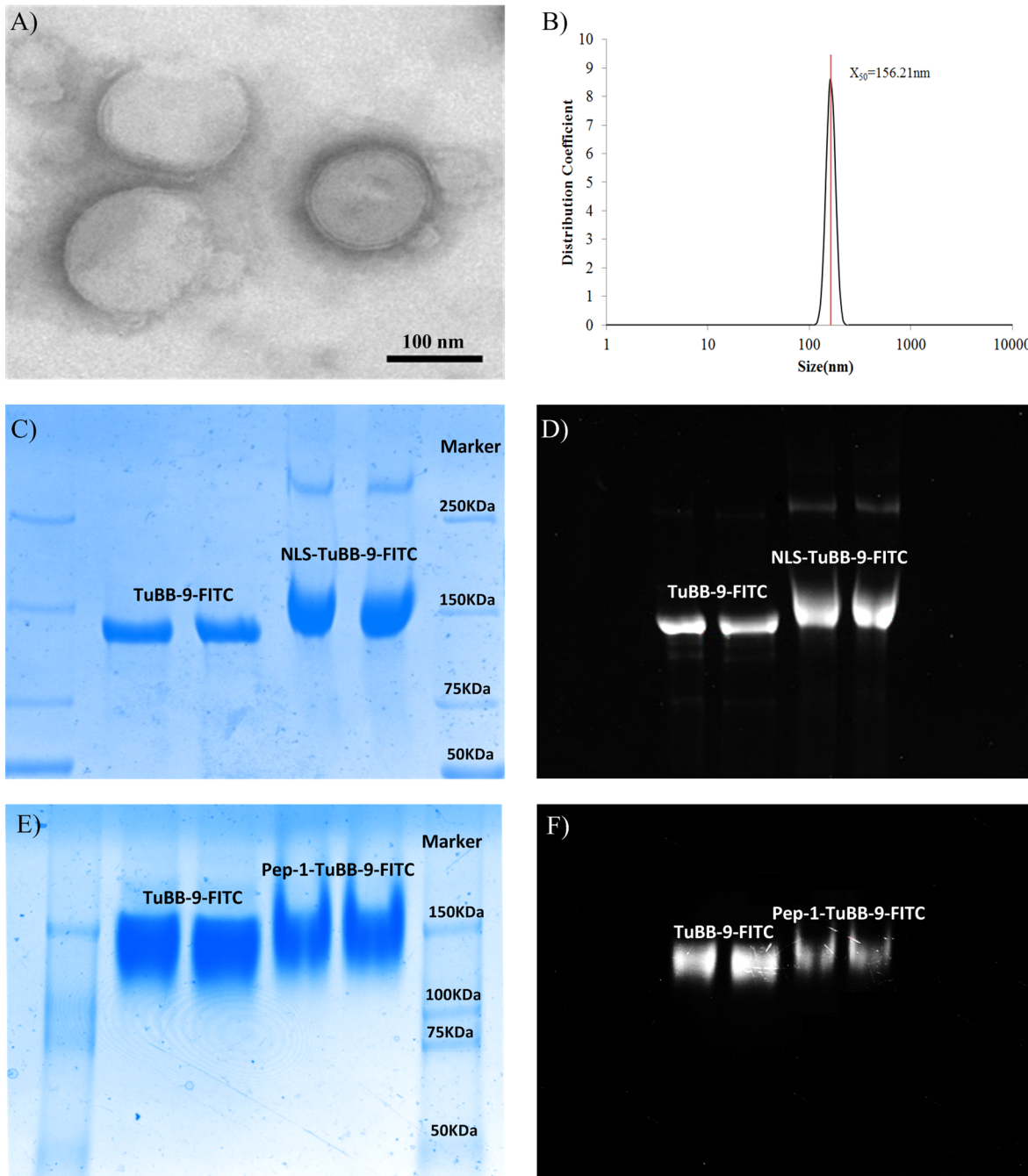


Figure 2. Characterization of the delivery constructs. (A) TEM images showed the bilayer structure of the liposomes. (B) DLS measurements proved a median size of approximately 160 nm of the liposomes. (C) SDS-PAGE gels (Coomassie Staining) with TuBB-9-FITC and NLS-TuBB-9-FITC demonstrated successful conjugation of NLS to TuBB-9-FITC. The shift in molecular weight from 138 kDa for TuBB-9-FITC to 141–153 kDa for NLS-TuBB-9-FITC corresponds with 2–10 NLS-peptides per antibody. (D) Fluorescence imaging of the gel proved the stable conjugation and fluorescence activity of FITC in NLS-TuBB-9-FITC. (E) Native-PAGE gels with TuBB-9-FITC and Pep-1-TuBB-9-FITC demonstrated after Coomassie Staining successful conjugation of Pep-1 to TuBB-9-FITC. (F) Fluorescence imaging of the gel demonstrates the stable conjugation and fluorescence activity of FITC in Pep-1-TuBB-9-FITC.

3. RESULTS

3.1. Characterization of Liposomal L-TuBB-9-FITC and NLS-TuBB-9-FITC.

The liposomes which encapsulated TuBB-9-FITC antibody-conjugates had a bilayer structure similar to cell membranes with a diameter of above 100 nm as proved by TEM imaging (Figure 2A). A narrow size distribution with a median diameter of 160 nm was confirmed by dynamic light scattering (DLS) (Figure 2B).

NLS-TuBB-9-FITC constructs were analyzed by SDS-PAGE to estimate the number of NLS-peptides conjugated to each molecule of TuBB-9-FITC. As shown in Figures 2C and 2D with Coomassie Blue staining of proteins and fluorescence imaging of FITC, the band of NLS-TuBB-9-FITC has a distinctly longer moving distance than TuBB-9-FITC only. The molecular weight of the antibody constructs increased from 138 kDa for TuBB-9-FITC to 141–153 kDa for NLS-TuBB-9-FITC. This difference corresponds with 2–10 NLS-peptides

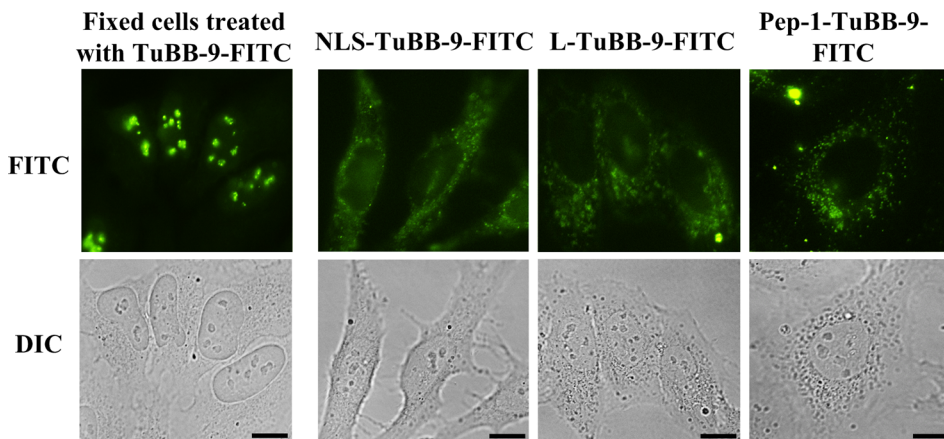


Figure 3. Nucleolar localization was not observed, when HeLa cells were incubated for 24 h with NLS-TuBB-9-FITC, L-TuBB-9-FITC, or Pep-1-TuBB-9-FITC. Immunostaining of fixed cells shows the typical pattern of the Ki-67 protein in the nucleoli (very right panel). Size bars: 10 μm .

with a molecular weight of 1.49 kDa incorporated into each molecule of TuBB-9-FITC.

Pep-1-TuBB-9-FITC constructs were analyzed by native-PAGE using Coomassie Blue staining (Figure 2E,F). The Pep-1-TuBB-9-FITC band has a distinct shorter moving distance than TuBB-9-FITC only. The molecular weight of the antibody constructs increased from 138 kDa for TuBB-9-FITC to about 142–149 kDa for Pep-1-TuBB-9-FITC. This difference corresponds with about 1–4 Pep-1 peptides with a molecular weight of 3 kDa incorporated into each molecule of TuBB-9-FITC.

3.2. Cellular Uptake and Localization of TuBB-9-FITC Constructs.

Intracellular localization of the constructs was observed by epifluorescence microscopy after an incubation period of 24 h with HeLa cells. All three TuBB-9-FITC constructs showed predominantly a punctured distribution in the cytoplasm, often with perinuclear accumulation (Figure 3). Staining patterns were completely different from the nucleolar localization of TuBB-9-FITC observed after staining of fixed cells. This suggests that the antibody constructs were taken up by endocytosis and to a large extent remain trapped inside the endolysosomal pathway. This endosomal entrapment was observed in all three tested cell lines HeLa, OVCAR-3, and human fibroblasts (Figure S1).

The uptake efficiency of the three TuBB-9-FITC constructs was measured as the total fluorescence intensity of cell lysates after 4 h incubation. Fluorescence of lysed HeLa cells was compared with the fluorescence of known amounts of constructs added to the cells in order to calculate the cellular uptake (Figure 4). The highest amount of uptake was observed in HeLa cells incubated with Pep-1-TuBB-9-FITC followed by L-TuBB-9-FITC and NLS-TuBB-9-FITC. As expected the least efficient uptake was observed with the labeled antibody alone.

3.3. Photochemically Triggered Release of Entrapped Antibody Conjugates.

Endolysosomal entrapped TuBB-9-FITC constructs were delivered to the cytosol by incubation with BPD and irradiation at 690 nm. To ensure the localization of BPD in HeLa cells at the site of the TuBB-9 constructs, fluorescence images of cells that were incubated with BPD for 22 h and TuBB-9-FITC constructs for 4 h were captured. BPD localizes mainly in mitochondria. Nevertheless it has been also reported to localize in the cytoplasm.³⁰ Figure 5 shows diffuse BPD fluorescence in the cytoplasm and partial colocalization of

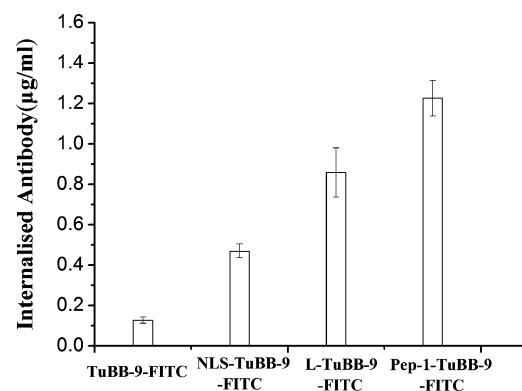


Figure 4. Uptake of TuBB-9-FITC in HeLa cells is highest with Pep-1-TuBB-9. After 4 h incubation with the conjugates, cells were lysed and the amount of antibodies was calculated by fluorescence spectroscopy.

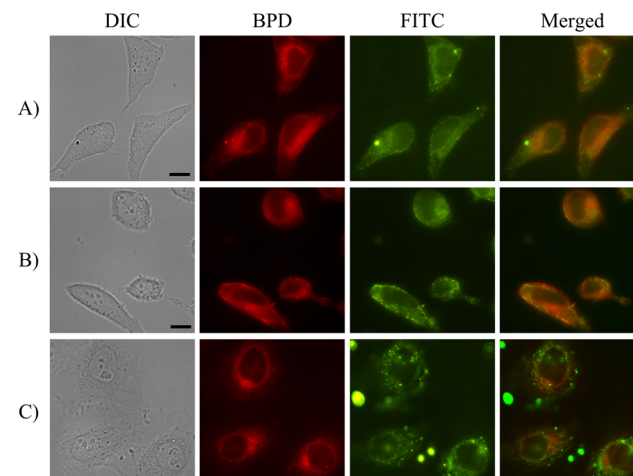


Figure 5. Partial colocalization of BPD with all three TuBB-9-FITC constructs was observed in HeLa cells. Cells were incubated with BPD for 18 h and with L-TuBB-9-FITC (A), NLS-TuBB-9-FITC (B), and Pep-1-TuBB-9-FITC (C) for another 4 h. Colocalization is seen in yellow in the merged images. Size bars: 10 μm .

BPD with the TuBB-9-FITC constructs. This colocalization seems to be weaker with the Pep-1 constructs. In addition, images of Pep-1 constructs show larger fluorescent spots, most likely occurring from aggregations of TuBB-9-FITC (Figure

5C, right panel). At 690 nm the photosensitizer BPD is efficiently excited without activating FITC (see Figure S2). Five minutes after irradiation, for all three TuBB-9-FITC constructs FITC fluorescence spread out from the dotted pattern observed before irradiation throughout the cytosol, into a more or less homogeneous fluorescence. 48 h after irradiation, the FITC signal is localized inside the nucleoli of the cells (Figure 6, and

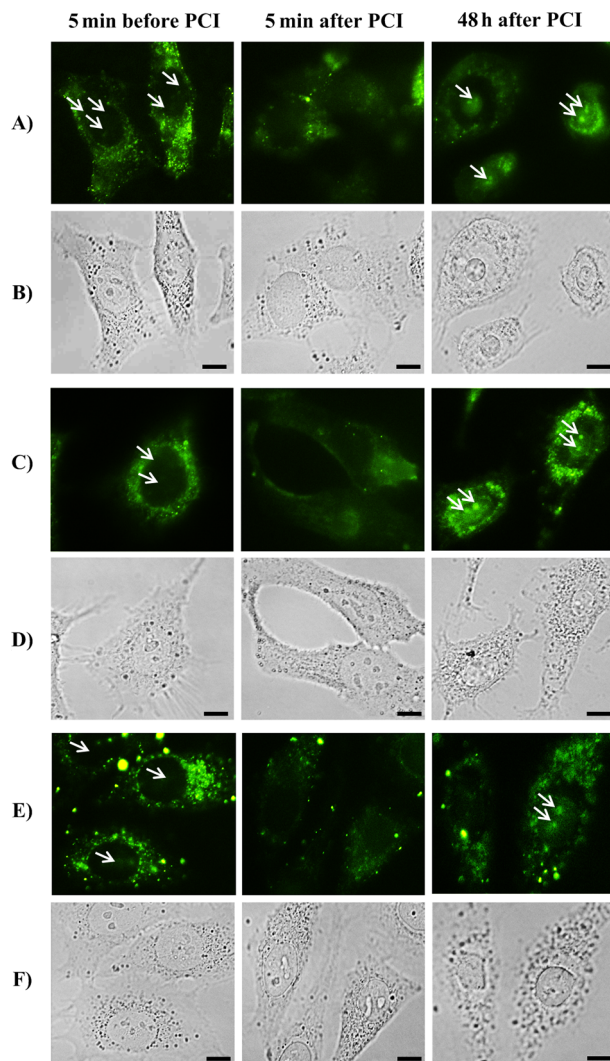


Figure 6. Nucleolar localization of TuBB-9-FITC can be observed in HeLa cells 48 h after BPD activation by 690 nm irradiation for all three constructs. Already 5 min after irradiation the FITC signal spread from the dotted distribution before irradiation throughout the cytosol. Cells were incubated with L-TuBB-9-FITC (A, B), NLS-TuBB-9-FITC (C, D), and Pep-1-TuBB-9-FITC (E, F). Arrows in fluorescence images point to the localization of nucleoli. Before PCI means 5 min before PCI irradiation after cells were incubated for 22 h with BPD and for 4 h with TuBB-9-FITC conjugates. Size bars: 10 μ m.

Figure S3, which includes also images taken 24 h after irradiation). A similar relocalization from the cytosol to the nucleus was observed after cytosolic microinjection.¹² The highest efficiency of nucleolar localization of the antibody after endolysosomal escape was found in the cells treated with NLS-TuBB-9-FITC (70%), followed by the liposomal construct L-TuBB-9-FITC where 66% of cells showed the typical Ki-67 staining pattern in the nucleoli. Flow cytometric measurements show that 90% of the HeLa cells are positive for Ki-67 (see

Figure S4). This means that at the maximum 90% of the cells can show nucleolar localization of the TuBB-9-FITC conjugates and therefore corresponds with nucleolar localization in 78% (70%/0.9) of Ki-67 positive cells for NLS-TuBB-9-FITC and 73% (66%/0.9) of Ki-67 positive cells for L-TuBB-9-FITC.

3.4. In Vitro Cytotoxicity Assay. Our previous studies demonstrated the ability of TuBB-9 conjugated to FITC to kill proliferating cancer cells after irradiation at 490 nm. The irradiation of TuBB-9-FITC leads to an inactivation of the Ki-67 protein or a binding partner and subsequent cell death.¹³ To evaluate the efficiency of TuBB-9-FITC constructs exerting their action after the dual irradiation at 690 and 490 nm, an in vitro cytotoxicity assay was performed. Figure 7 shows the cytotoxic effects of L-TuBB-9-FITC (Figure 7A), NLS-TuBB-9-FITC (Figure 7B), and Pep-1-TuBB-9-FITC (Figure 7C). For control measurements TuBB-9 was exchanged by the EGFR-binding antibody Erbitux. Besides L-TuBB-9-FITC, NLS-TuBB-9-FITC, and Pep-1-TuBB-9-FITC, also plain TuBB-9-FITC and incubation only with BPD served as controls. Although most of the damaging effects were limited to the endosomal membrane, all the groups treated with BPD showed a loss in cell viability of approximately 20% after 690 nm irradiation. This represents the unspecific effect from PCI irradiation with BPD. Irradiation at 490 nm only decreased cell viability also slightly for 10–20%. However, groups treated with TuBB-9-FITC constructs and irradiated at 690 and 490 nm irradiation showed the most efficient cell killing. Differences in cell viability were observed between the TuBB-9-FITC constructs, TuBB-9-FITC only, and Erbitux-FITC constructs. Among the three different TuBB-9-FITC constructs, the NLS-TuBB-9-FITC showed the highest cell killing efficiency (cell viability of 13% \pm 4%), compared to the group treated with the liposomal L-TuBB-9-FITC (18% \pm 7%) or with Pep-1-TuBB-9-FITC (28% \pm 7%).

Live/dead fluorescence staining with calcein AM and propidium iodide showed highly efficient cell killing after irradiation at 690 and 490 nm (Figure 8).

Also growth curves of the treated cells illustrate the strong decrease in cell viability after light activated release by 690 nm irradiation and photochemical activation of FITC by 490 nm irradiation (Figure 9). NLS-TuBB-9-FITC and L-TuBB-9-FITC conjugates not only decrease cell number but also delay regrowth from the surviving cell fraction within the studied time period, 10 days.

4. DISCUSSION

Effective intracellular delivery and the overcoming of endosomal entrapment of macromolecular agents are major challenges in molecular therapies aimed at intracellular targets. In this study we show that an effective light induced endosomal escape allows successful delivery of the Ki-67 antibody TuBB-9 to the cell nucleus. Vehicles for intracellular delivery are important for an effective targeting strategy, but do not always lead to a free cytoplasmic availability. An effective endosomal escape mechanism leaves more options for the choice of the delivery vehicles. All three TuBB-9-FITC constructs for intracellular delivery, i.e., liposomes, a covalently linked NLS peptide, and a commercially available noncovalently linked protein transfection system (Pep-1 peptide), were taken up by the cells in varying but nonetheless relatively high amounts. But the characteristic Ki-67 staining pattern was observed only in a small number of cells. Instead the fluorescence of the constructs was found to be distributed in point-like structures in the

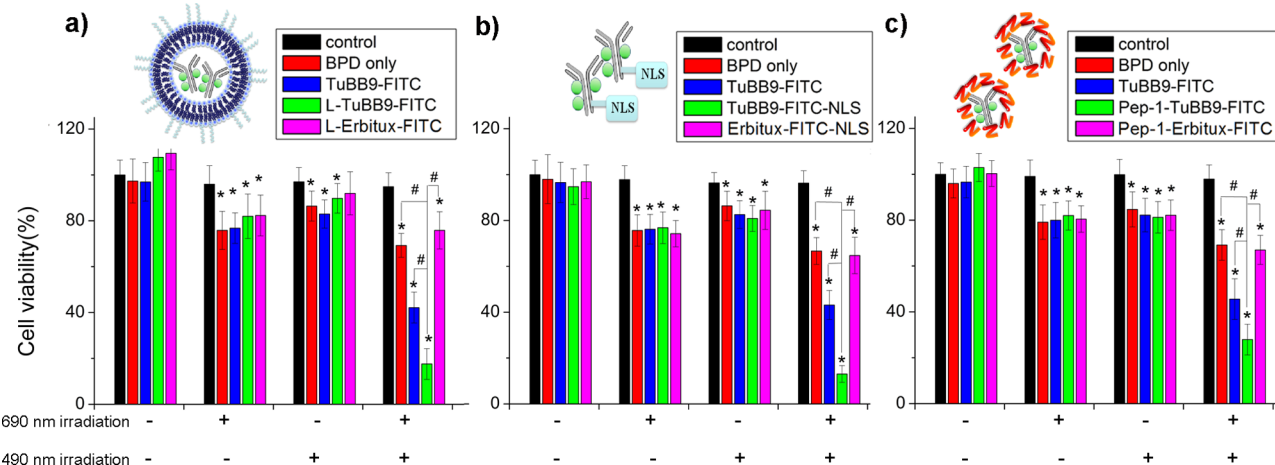


Figure 7. Selective elimination of proliferating cells by TuBB-9-FITC. Dual irradiation at 690 and 490 nm caused endoplasmatic release and inactivation of Ki-67. HeLa cells were incubated with (A) L-TuBB-9-FITC, (B) NLS-TuBB-9-FITC, and (C) Pep-1-TuBB-9-FITC. The highest effect was observed for delivery by NLS sequence or the liposome. The symbol * indicates statistically significant difference in cell viability between samples and control after *t*-test analysis ($p < 0.05$); the symbol # indicates statistically significant difference in cell viability between two linked samples after *t*-test analysis ($p < 0.05$).

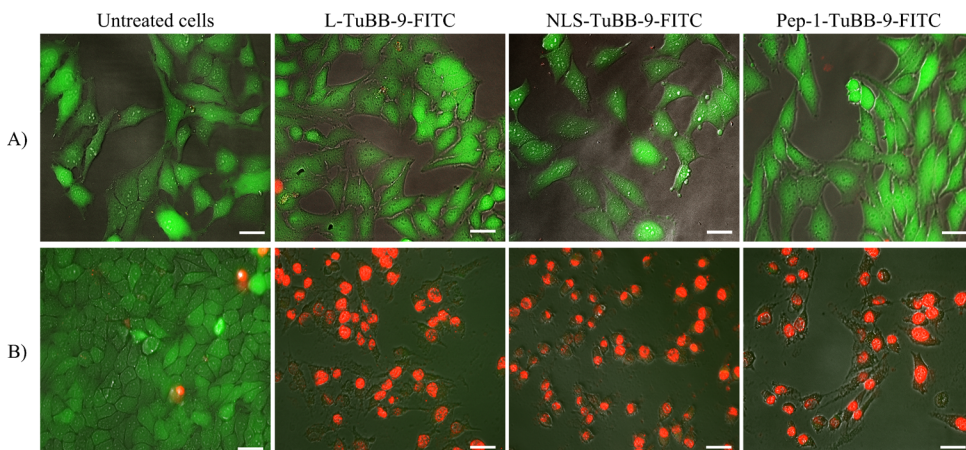


Figure 8. Live/dead staining shows the selective elimination of proliferating cells by TuBB-9-FITC. HeLa cells were incubated with BPD and with L-TuBB-9-FITC, NLS-TuBB-9-FITC, and Pep-1-TuBB-9-FITC as indicated. Cells were stained with calcein AM (green) and propidium iodide (red) before irradiation (A) and after irradiation at 690 and 490 nm (B). Size bars: 30 μ m.

cytoplasm of HeLa or OVCAR-3 cells, which indicates that the TuBB-9-FITC was trapped in endosomal compartments. Incubation with BPD and irradiation at 690 nm led to an escape of the trapped antibodies from endosomes and a spreading of the conjugates into the cytoplasm. 24 h and 48 h after irradiation, the FITC fluorescence of the nucleoli demonstrated successful binding to Ki-67. The relocalization of the antibody from the cytosol to the nucleus is presumably due to cotransport of the antibody with newly synthesized Ki-67 protein, or due to binding to Ki-67 during mitosis after breakdown of the nuclear envelope. The irradiation with 490 nm at this stage photochemically cross-linked Ki-67 with interacting or nearby biomolecules,¹² resulting in cell death.¹³ Although Pep-1-TuBB-9-FITC showed the highest uptake efficiency, the efficiency of cell elimination was the lowest among the three constructs. The lower cell elimination efficiency for Pep-1-TuBB-9-FITC can be explained by aggregation, which can be seen as large fluorescing extracellular structures (Figure 3 (very right panel), Figures 5C, 6E). The aggregates may hinder TuBB-9 from binding to the Ki-67 protein and reduce the amount of active conjugates. Best cell

killing results were obtained with NLS-TuBB-9-FITC and L-TuBB-9-FITC. The covalent linkage of the NLS may help to deliver the antibody more effectively to the cell nucleus in a higher number of cells.

Selective photochemical destruction of endosomes has also been described as photochemical internalization (PCI)^{21,29,31,32} and has originally been developed from photodynamic therapy (PDT) of tumors, which uses the production of reactive oxygen species from a photosensitizer to destroy unwanted cells.^{33,34} For PCI much lower concentrations of the photosensitizers and lower light doses are applied to restrict the photochemical effect to endosomes. Nevertheless PCI has also potential toxic effects on cells. In our study at the low photosensitizer and light doses used, a certain degree of cell toxicity was observed, when cells were only incubated with BPD and irradiated at 690 nm. For successful endosomal escaping, the balance of cell damage and the efficiency of the endosomal escape can probably be further improved by a choice of different irradiation time point and photosensitizer. More amphiphilic photosensitizers like the PS Amphinex (TPCS_{2a}) seem to be better suited for PCI and are,

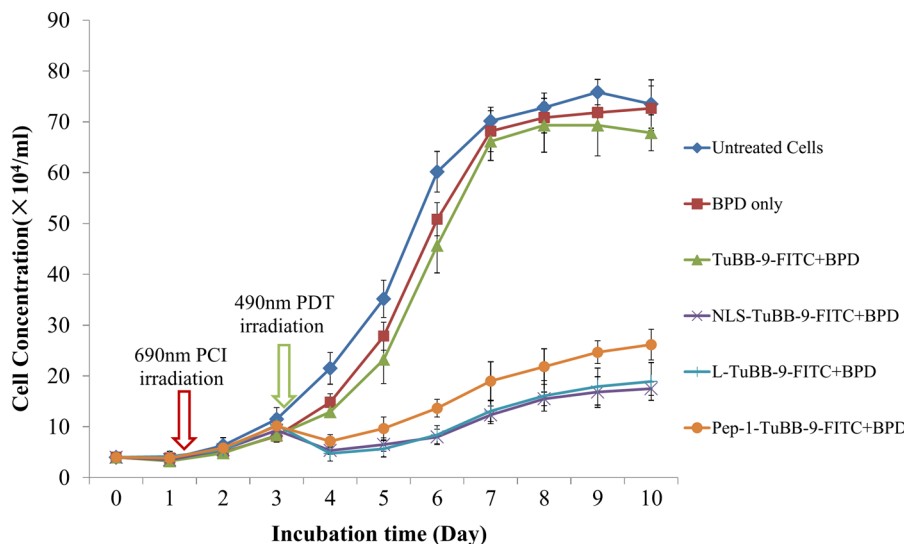


Figure 9. Growth curves of treated HeLa cells showed decrease in cell viability after irradiations and delayed regrowth of the surviving cell fraction. HeLa cells were incubated with L-TuBB-9-FITC, NLS-TuBB-9-FITC, and Pep-1-TuBB-9-FITC; control samples include cells only, cells incubated with BPD, and cells incubated with TuBB-9-FITC.

in combination with bleomycin, already in clinical phase II studies for the treatment of head and neck cancer.³⁵

Our study shows that, without forced endosomal escape, internalized antibody conjugates can hardly pass out of the endolysosomal pathway and reach the target destination. Thus, high concentrations of protein or antibody cargoes are needed, if intracellular targeting should work at all. Improving the intracellular availability by PCI will diminish in clinical applications the agent concentration in the circulation and thereby reduce toxic side effects to a patient. Therefore, methods for endosomal release are crucial to optimize selectivity. In our hands PCI was a fast and stable tool to effectively target Ki-67 with very low doses of antibody conjugates.

BPD and FITC have both been used as fluorescent and photosensitizing dyes. BPD is broadly used in photodynamic therapy and is clinically approved for the treatment of age related macular degeneration (AMD).^{36,37} BPD has a high singlet oxygen yield of over 80% in aqueous solution.³⁸ FITC has been used, besides for fluorescent imaging, for protein inactivation in an approach also named chromophore assisted light inactivation (CALI).³⁹ The inactivation of surrounding proteins involves photo-cross-linking after oxidation of methionine side chains.⁴⁰ Although FITC has a singlet oxygen quantum yield of only 3% in aqueous solution, it has a higher absorption cross-section. The conjugation to antibodies may in addition alter its photophysical properties in favor of a photochemical action. For protein inactivation it is an effective agent similar to malachite and indocyanine green.^{41,42}

Compared to therapeutic antibodies, which only block receptors by binding, inhibition of cell growth by photochemical Ki-67 targeting is expected to be achievable at considerably lower antibody concentrations. Erbitux is clinically used in cancer therapy to decrease proliferation of EGFR overexpressing cancer cells.⁴³ At the low antibody concentrations (100 nM) used in these experiments, Erbitux could even be used as a control antibody, since it did not show any effects on cell viability, with or without light irradiation. In contrast, the Ki-67 binding antibody TuBB-9-FITC led at 100 nM concentration to a selective and prominent cell death after

irradiation. The two photochemical steps that we introduced here not only provide additional selectivity by limiting effects to irradiated areas but also drastically reduce the amount of administered antibodies.

In conclusion, our study shows a new light-triggered strategy to effectively target proteins in the cell nucleus. We showed an efficient intracellular delivery of antibody conjugates that are freely available in the cytosol and their successful transport to the nucleus. The synergistic effect of PCI irradiation and PDT irradiation with the nuclear target Ki-67 led to efficient cell death with molecular selectivity. Liposomal or peptide triggered delivery shows similar results, leading to the conclusion that an effective strategy for endosomal escape leaves greater variability for the choice of the delivery agent.

For in vivo application many additional factors, like the serum distribution and pharmacokinetics, have to be considered. Optimal concentration, delivery vehicle, irradiation time points, and light dose may be different. Animal studies are under way to address these points and to prove our concept of selective photochemical targeting of proliferating cells in small animals.

ASSOCIATED CONTENT

Supporting Information

The Supporting Information is available free of charge on the ACS Publications website at DOI: [10.1021/acs.molpharmaceut.5b00260](https://doi.org/10.1021/acs.molpharmaceut.5b00260).

[Additional figures \(PDF\)](#)

AUTHOR INFORMATION

Corresponding Author

*Tel: +49 451 5006511. E-mail: rahmanzadeh@bmo.uni-luebeck.de.

Notes

The authors declare no competing financial interest.

[§]The work by S.W. was performed at the Institute of Biomedical Optics, University of Lübeck, in the framework of the joint Ph.D. program sponsored by the China Scholarship Council.

ACKNOWLEDGMENTS

This work was supported by the German Research Foundation (DFG, Grant No. Ra1771/3-1) and The National Natural Science Foundation of China (No. 61120106013).

REFERENCES

- (1) Sawyers, C. Targeted cancer therapy. *Nature* **2004**, *432* (7015), 294–297.
- (2) Imai, K.; Takaoka, A. Comparing antibody and small-molecule therapies for cancer. *Nat. Rev. Cancer* **2006**, *6* (9), 714–727.
- (3) Diaz, L. A., Jr; Williams, R. T.; Wu, J.; Kinde, I.; Hecht, J. R.; Berlin, J.; Allen, B.; Bozic, I.; Reiter, J. G.; Nowak, M. A.; Kinzler, K. W.; Oliner, K. S.; Vogelstein, B. The molecular evolution of acquired resistance to targeted EGFR blockade in colorectal cancers. *Nature* **2012**, *486* (7404), 537–540.
- (4) Arteaga, C. L.; Sliwkowski, M. X.; Osborne, C. K.; Perez, E. A.; Puglisi, F.; Gianni, L. Treatment of HER2-positive breast cancer: current status and future perspectives. *Nat. Rev. Clin. Oncol.* **2011**, *9* (1), 16–32.
- (5) Smith, B.; Lyakhov, I.; Loomis, K.; Needle, D.; Baxa, U.; Yavlovich, A.; Capala, J.; Blumenthal, R.; Puri, A. Hyperthermia-triggered intracellular delivery of anticancer agent to HER2(+) cells by HER2-specific affibody (ZHER2-GS-Cys)-conjugated thermosensitive liposomes (HER2(+) affisomes). *J. Controlled Release* **2011**, *153* (2), 187–194.
- (6) Sia, D.; Alsinet, C.; Newell, P.; Villanueva, A. VEGF signaling in cancer treatment. *Curr. Pharm. Des.* **2014**, *20* (17), 2834–2842.
- (7) Sharei, A.; Zoldan, J.; Adamo, A.; Sim, W. Y.; Cho, N.; Jackson, E.; Mao, S.; Schneider, S.; Han, M.-J.; Lytton-Jean, A. A vector-free microfluidic platform for intracellular delivery. *Proc. Natl. Acad. Sci. U. S. A.* **2013**, *110* (6), 2082–2087.
- (8) Gerdes, J.; Lemke, H.; Baisch, H.; Wacker, H.-H.; Schwab, U.; Stein, H. Cell cycle analysis of a cell proliferation-associated human nuclear antigen defined by the monoclonal antibody Ki-67. *J. Immunol.* **1984**, *133* (4), 1710–1715.
- (9) Gerdes, J.; Schwab, U.; Lemke, H.; Stein, H. Production of a mouse monoclonal antibody reactive with a human nuclear antigen associated with cell proliferation. *Int. J. Cancer* **1983**, *31* (1), 13–20.
- (10) Scholzen, T.; Gerdes, J. The Ki-67 protein: from the known and the unknown. *J. Cell. Physiol.* **2000**, *182* (3), 311–322.
- (11) Bullwinkel, J.; Baron-Lühr, B.; Lüdemann, A.; Wohlenberg, C.; Gerdes, J.; Scholzen, T. Ki-67 protein is associated with ribosomal RNA transcription in quiescent and proliferating cells. *J. Cell. Physiol.* **2006**, *206* (3), 624–635.
- (12) Rahmazadeh, R.; Hüttmann, G.; Gerdes, J.; Scholzen, T. Chromophore-assisted light inactivation of pKi-67 leads to inhibition of ribosomal RNA synthesis. *Cell Proliferation* **2007**, *40* (3), 422–430.
- (13) Rahmazadeh, R.; Rai, P.; Celli, J. P.; Rizvi, I.; Baron-Lühr, B.; Gerdes, J.; Hasan, T. Ki-67 as a molecular target for therapy in an in vitro three-dimensional model for ovarian cancer. *Cancer Res.* **2010**, *70* (22), 9234–9242.
- (14) Deshayes, S.; Morris, M.; Divita, G.; Heitz, F. Cell-penetrating peptides: tools for intracellular delivery of therapeutics. *Cell. Mol. Life Sci.* **2005**, *62* (16), 1839–1849.
- (15) Ladmiral, V.; Semsarilar, M.; Canton, I.; Armes, S. P. Polymerization-induced self-assembly of galactose-functionalized biocompatible diblock copolymers for intracellular delivery. *J. Am. Chem. Soc.* **2013**, *135* (36), 13574–13581.
- (16) Kondo, Y.; Miyata, K.; Kato, F. Efficient delivery of antibody into living cells using hemagglutinating virus of Japan (HVJ) envelope. *Curr. Protoc. Immunol.* **2010**, DOI: 10.1002/0471142735.im0216s89.
- (17) Canton, I.; Massignani, M.; Patikarnmonthon, N.; Chierico, L.; Robertson, J.; Renshaw, S. A.; Warren, N. J.; Madsen, J. P.; Armes, S. P.; Lewis, A. L. Fully synthetic polymer vesicles for intracellular delivery of antibodies in live cells. *FASEB J.* **2013**, *27* (1), 98–108.
- (18) Yan, M.; Du, J.; Gu, Z.; Liang, M.; Hu, Y.; Zhang, W.; Priceman, S.; Wu, L.; Zhou, Z. H.; Liu, Z. A novel intracellular protein delivery platform based on single-protein nanocapsules. *Nat. Nanotechnol.* **2010**, *5* (1), 48–53.
- (19) Futaki, S.; Hirose, H.; Nakase, I. Arginine-rich peptides: methods of translocation through biological membranes. *Curr. Pharm. Des.* **2013**, *19* (16), 2863–2868.
- (20) Shete, H. K.; Prabhu, R. H.; Patravale, V. B. Endosomal Escape: A Bottleneck in Intracellular Delivery. *J. Nanosci. Nanotechnol.* **2014**, *14* (1), 460–474.
- (21) Varkouhi, A. K.; Scholte, M.; Storm, G.; Haisma, H. J. Endosomal escape pathways for delivery of biologicals. *J. Controlled Release* **2011**, *151* (3), 220–228.
- (22) Bozzuto, G.; Molinari, A. Liposomes as nanomedical devices. *Int. J. Nanomed.* **2015**, *10*, 975–99.
- (23) Morris, M. C.; Depollier, J.; Mery, J.; Heitz, F.; Divita, G. A peptide carrier for the delivery of biologically active proteins into mammalian cells. *Nat. Biotechnol.* **2001**, *19* (12), 1173–1176.
- (24) Costantini, D. L.; Villani, D. F.; Vallis, K. A.; Reilly, R. M. Methotrexate, Paclitaxel, and Doxorubicin Radiosensitize HER2-Amplified Human Breast Cancer Cells to the Auger Electron-Emitting Radiotherapeutic Agent 111In-NLS-Trastuzumab. *J. Nucl. Med.* **2010**, *51* (3), 477–483.
- (25) Ezzeddine, R.; Al-Banaw, A.; Tovmasyan, A.; Craik, J. D.; Batinic-Haberle, I.; Benov, L. T. Effect of molecular characteristics on cellular uptake, subcellular localization, and phototoxicity of Zn(II) N-alkylpyridylporphyrins. *J. Biol. Chem.* **2013**, *288* (51), 36579–88.
- (26) Aveline, B.; Hasan, T.; Redmond, R. W. Photophysical and photosensitizing properties of benzoporphyrin derivative monoacid ring A (BPD-MA). *Photochem. Photobiol.* **1994**, *59* (3), 328–35.
- (27) Moan, J.; Berg, K. The photodegradation of porphyrins in cells can be used to estimate the lifetime of singlet oxygen. *Photochem. Photobiol.* **1991**, *53* (4), 549–53.
- (28) Prasmickaite, L.; Høgset, A.; Selbo, P.; Engesæter, B. Ø.; Hellum, M.; Berg, K. Photochemical disruption of endocytic vesicles before delivery of drugs: a new strategy for cancer therapy. *Br. J. Cancer* **2002**, *86* (4), 652–657.
- (29) Chen, P.; Wang, J.; Hope, K.; Jin, L.; Dick, J.; Cameron, R.; Brandwein, J.; Minden, M.; Reilly, R. M. Nuclear localizing sequences promote nuclear translocation and enhance the radiotoxicity of the anti-CD33 monoclonal antibody HuM195 labeled with 111In in human myeloid leukemia cells. *J. Nucl. Med.* **2006**, *47* (5), 827–36.
- (30) Runnels, J. M.; Chen, N.; Ortel, B.; Kato, D.; Hasan, T. BPD-MA-mediated photosensitization in vitro and in vivo: cellular adhesion and beta1 integrin expression in ovarian cancer cells. *Br. J. Cancer* **1999**, *80* (7), 946–53.
- (31) Selbo, P. K.; Weyergang, A.; Høgset, A.; Norum, O.-J.; Berstad, M. B.; Vikdal, M.; Berg, K. Photochemical internalization provides time-and space-controlled endolysosomal escape of therapeutic molecules. *J. Controlled Release* **2010**, *148* (1), 2–12.
- (32) Lee, C. S.; Park, W.; Park, S. J.; Na, K. Endolysosomal environment-responsive photodynamic nanocarrier to enhance cytosolic drug delivery via photosensitizer-mediated membrane disruption. *Biomaterials* **2013**, *34* (36), 9227–36.
- (33) Solban, N.; Rizvi, I.; Hasan, T. Targeted photodynamic therapy. *Lasers Surg. Med.* **2006**, *38* (5), 522–31.
- (34) Agostinis, P.; Berg, K.; Cengel, K. A.; Foster, T. H.; Girotti, A. W.; Gollnick, S. O.; Hahn, S. M.; Hamblin, M. R.; Juzeniene, A.; Kessel, D.; Korbelik, M.; Moan, J.; Mroz, P.; Nowis, D.; Piette, J.; Wilson, B. C.; Golab, J. Photodynamic therapy of cancer: an update. *Ca-Cancer J. Clin.* **2011**, *61* (4), 250–81.
- (35) Berg, K.; Nordstrand, S.; Selbo, P. K.; Tran, D. T. T.; Angell-Petersen, E.; Høgset, A. Disulfonated tetraphenyl chlorin (TPCS 2a), a novel photosensitizer developed for clinical utilization of photochemical internalization. *Photochem. Photobiol. Sci.* **2011**, *10* (10), 1637–1651.
- (36) Schmidt-Erfurth, U.; Hasan, T. Mechanisms of action of photodynamic therapy with verteporfin for the treatment of age-related macular degeneration. *Surv. Ophthalmol.* **2000**, *45* (3), 195–214.

- (37) Schmidt-Erfurth, U.; Hasan, T.; Schomacker, K.; Flotte, T.; Birngruber, R. In vivo uptake of liposomal benzoporphyrin derivative and photothrombosis in experimental corneal neovascularization. *Lasers Surg. Med.* **1995**, *17* (2), 178–88.
- (38) Redmond, R. W.; Gamlin, J. N. A compilation of singlet oxygen yields from biologically relevant molecules. *Photochem. Photobiol.* **1999**, *70* (4), 391–475.
- (39) Hoffman-Kim, D.; Diefenbach, T. J.; Eustace, B. K.; Jay, D. G. Chromophore-assisted laser inactivation. *Methods Cell Biol.* **2007**, *82*, 335–54.
- (40) Yan, P.; Xiong, Y.; Chen, B.; Negash, S.; Squier, T. C.; Mayer, M. U. Fluorophore-Assisted Light Inactivation of Calmodulin Involves Singlet-Oxygen Mediated Cross-Linking and Methionine Oxidation. *Biochemistry* **2006**, *45*, 4736–4748.
- (41) Liao, J. C.; Roider, J.; Jay, D. G. Chromophore-assisted laser inactivation of proteins is mediated by the photogeneration of free radicals. *Proc. Natl. Acad. Sci. U. S. A.* **1994**, *91* (7), 2659–2663.
- (42) Surrey, T.; Elowitz, M. B.; Wolf, P. E.; Yang, F.; Nedelec, F.; Shokat, K.; Leibler, S. Chromophore-assisted light inactivation and self-organization of microtubules and motors. *Proc. Natl. Acad. Sci. U. S. A.* **1998**, *95* (8), 4293–4298.
- (43) Jackson, S. E.; Chester, J. D. Personalised cancer medicine. *Int. J. Cancer* **2015**, *137* (2), 262–6.